Effects of Multi-stack Ball Grid Array on Multi-stack Printed Circuit Board

IOP Conf. Series: Materials Science and Engineering **530** (2019) 012017 doi:10.1088/1757-899X/530/1/012017

Effects of Multi-stack Ball Grid Array on Multi-stack Printed Circuit Board

M A F M Mukhtar[1*], A Abas[2], W M E I W S Bahri[1]

[1]DRB Hicom University of Automotive Malaysia (DHU), Lot 1449, PT 2204 Peramu Jaya Industrial Area 26607 Pekan, Pahang Darul Makmur, Malaysia.

[2]Universiti Sains Malaysia, 11800 Gelugor, Penang, Malaysia

Corresponding author *: fatah@dhu.edu.my

Abstract. In the customary underfill (CUF) epitome process, there are couple of downsides experienced for instance, extended filling time, divided filling and voids improvement. Test and FVM reenactments have been directed to examine CUF dispensing systems for different types of ball grid array (BGA) tendencies out of a solitary layered PCB. In this task, the principle point is to enhance the stream of under filling mold crosswise over multi-stacks BGA. Package on Package (PoP), a strategy for coordinated circuit bundling, is utilized to consolidate BGA bundles vertically to permit higher segment thickness in devices. The L-type liquid stream in multi-stack BGA with edge introduction is contemplated and parameters of CUP exemplification, for example, void development and filling time were examined. The results demonstrated that the BGA sizes with the little weld balls put at the base layer, trailed by the medium size bind balls in the center stack and the biggest patch balls at the top layer has appeared to enhance the stream rate of the encapsulant ideally. Other arrangement in which the medium size solders placed are at the base layer, small solders at the center layer and largest solders on top of it, requires longest total filling time. The result also shows that the racing effect is present at central region and at the side of the layer. Because of the perimeter orientation design, the void formation is minimal and the race effect is not affecting much according experimental and computational result. This investigation additionally uncovers the capability of air gaps in improving velocity and pressure distribution near inlet and outlet to achieve faster total filling time at all layers of the BGA.

1. Introduction

Underfill encapsulation process is a process in which the space between the silicon die and the PCB is filled with the underfill encapsulant that redistributes the induced stress thereby enhancing the solder reliability [1-2]. This underfill process consists of apportioning a managed measure from fabric into an opening among chip and substrate. It is also determined crucial for ensuring and rising unwavering first-class of the digital packaging (EP). It can lessen the global thermal expansion, stresses and pressure within the silicon chip and substrate.Hole among the chip and silicon should totally dispatched with underfilling mildew for the purpose of making certain life of the chip meeting [4]. Affiliation among underfill mould and solder bumps may actuate doable void or air pocket formation and solder bump harmed because of inappropriate dedication of underfill material and processing parameter [2-5]. Thus, superior comprehension at underfilling process is critical and can be done through virtual modeling method [6-7].

In the stream of new technologies nowadays, Electronic industries are seeking for towards smaller scale electronic chip packaging process along with rises in functionality and the demand for multi stack chip is highly desirable[8]. Due to this matters, multi stack BGA are now being under researched. The

research that have been made by Bart et.al focuses on stress analysis through for the underfilling material and substrate [8]. Meanwhile, the simulation and experiment observation that were conducted by Abdullah et.al showed that the flow was halted as it flows over the chip due to tiny gap height. They also make a calculation to show that the minimum die top clearance is 0.25mm for flip chip to prevent from short shot issues [9]. In other research, Ernest et.al performed a research on flip chip with a series of experiments and simulations to handle the encapsulation flow and chip deformation. These researchers provide some insight on the stress distributions during the encapsulation process [10].

Based on the research that made by Chen et.al, thermal mode analysis is used to optimize thermal management to identify optimal locations and size of multi chip package. The average thermal resistance is analyzed throughout the investigations and found that thermal resistance matrix is independent of power dissipation [11].

This research, focuses on ball grid array (BGA) sizes effect to the fluid flow simulation. There are rarely research and investigation that has been conducted on the size variation of multi stacks BGA. The related Ansys software tutorials are studied to have an understanding on the fluid flow simulation. A modification is done on Ansys Fluent in order to generate the multi-stacks ball grid array (BGA) with perimeter orientation of spherical solder bump array subjected to fluid flow. Various parameters like filling time, flow front pattern, pressure and velocity dissemination are examined based on real world encapsulant liquid. A comparison is then made between simulation and experimental result of the fluid flow.

2. Methodology

2.1. Experiment Detail

In order to enhance the visualization aspect of the micro-sized package a scaled-up experiment is constructed. The BGA models are scaled-up by at least six-time bigger than the real ball grid array (BGA) size for ease of newability. The design parameters of the models are summarized in table 1.

Table 1: Parameter of BGA model

Parameter	**Actual size**	**Scale up size**
Parallel plates (mm)	Not applicable	108 (L) x 108 (W) x 5 (T)
Bump Diameter (mm)	0.5	2.9 and 5.5
Bump Pitch (mm)	1.0	5.8 and 11.0
Bump Height (mm)	0.495	2.4 and 4.9

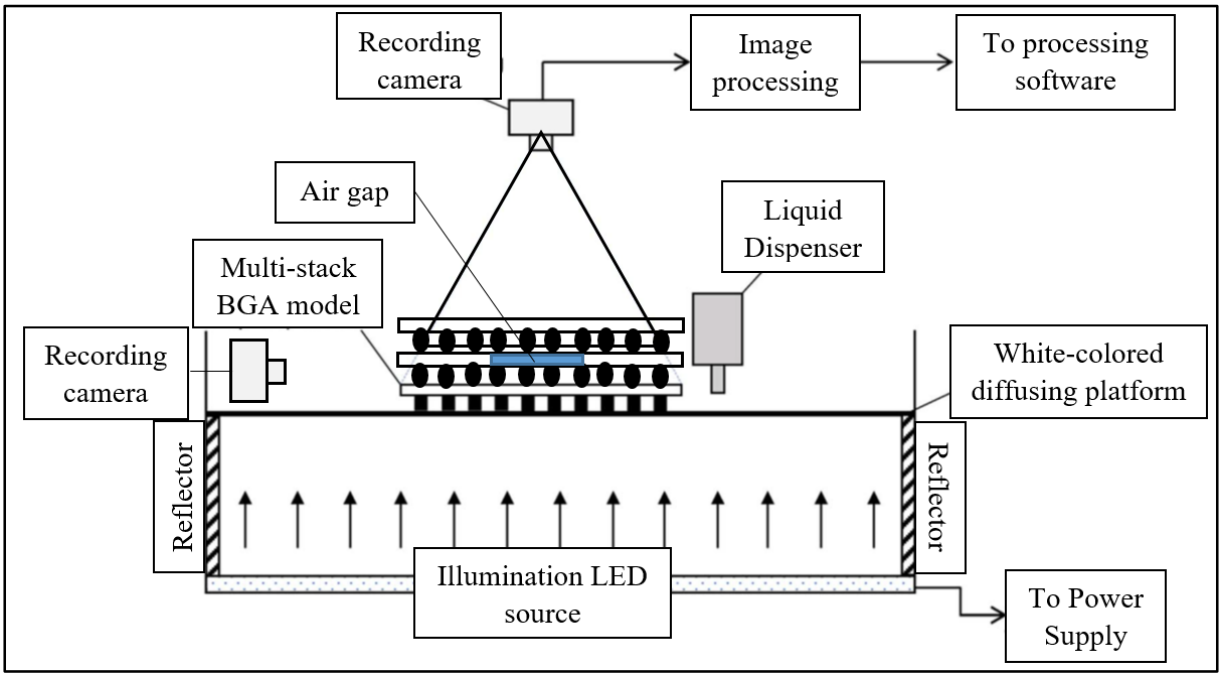

Figure 1: Schematic experimental scaled – up setup for the study of different size of multi stack ball grid array.

The epoxy-molded compound (EMC) used as the encapsulant material with its properties are summarized in Table 2 as stated below.

Table 2: EMC encapsulant material properties

Parameter	**Value**
Density (kg/m^3)	1843
Specific heat capacity (J/kg-K)	1163
Thermal conductivity (W/m-K)	0.8
Molecular weight (kg/kgmol)	44.05358
Dynamic Viscosity (Pa-s)	2.2
Kinematic viscosity (mm2/s)	2111.3
Standard state enthalpy (J/kgmol)	-1.653202e+08
Reference temperature (K)	298.00001

2.2. Numerical Simulations

2.2.1. Equations

2.2.1.1 Navier – Stokes Formulation. The governing equations based on Navier-Stokes equation is used to simulate the encapsulant material and air through the use of conservation of mass and momentum. In the encapsulation system, both fluids are assumed to be incompressible and laminar

Continuity equation:

$$\frac{\partial \rho}{\partial t} + +\nabla.(\rho\vec{u}) = 0 \quad (1)$$

Navier – stokes equation:

$$\frac{\partial}{\partial t}(\rho\vec{u}) + \nabla.(\rho\vec{u}\vec{u}) = -\nabla P + \nabla.\bar{\bar{\tau}} + \rho\vec{g} \quad (2)$$

In the version, EMC and air are differentiated using multiphase formulation. The quantity of fluids (VOF) for each levels is described the use of transport equation at the same time as the distribution of fluid is represented via quantity fraction, f in the range of zero <f <1. Generally, f=0 imply the absence of EMC whilst f=1 imply the cell is completely full of EMC.
Transport equation:

$$\frac{df}{dt} + \nabla.(\bar{u}f) = 0 \quad (3)$$

2.2.1.2 Capillary Force Formulation. The underfill fluid flows through the ball grid array (BGA) primarily based on the capillary motion without the assistance of the outside pressure. There are two regions in the fluid capillary waft movement which can be wetting and non-wetting fluid place. The underfill fluid is inside the non-wetting region.The capillary pressure is defined as the pressure difference between wetting and non-wetting fluid. The equivalence to atmospheric pressure can be considered since the non-wetting fluid is air.

$$Capillary\ Pressure, \qquad \Delta P_c = P_{nw} - P_w \quad (4)$$

$$= \frac{2\sigma}{b} \quad (5)$$

Where σ the fluid surface tension and b is is the gap height.

The equation 6 and 7 show that capillary pressure is proportional to surface tension and inversely proportional to the gap height. There are two conditions as shown below:

$$\Delta P_c > \frac{2\sigma}{b} \quad (6)$$

The pressure of non-wetting fluid is greater than the pressure of the wetting fluid. Thus, the fluid in non-wetting region will filled or move to the wetting region (underfilling process phenomenon).

$$\Delta P_c < \frac{2\sigma}{b} \quad (7)$$

The pressure of non-wetting fluid is lower than the pressure of the wetting fluid. Thus, the fluid in the non-wetting region will remain static.

3. Results & Discussion

3.1. Model validation

Two sets of experiments with different solder ball arrangements were carried out for a scaled-up BGA model. The top views of the model are recorded during the filling process of the viscous encapsulant

into the cavity in the L-type dispensing. The simulation results of the flow front profile obtained from simulation results were compared with the experimental results. Generally, judging from the observation for all two set of experiments of flow front profile, it shows a good relation between the experimental works and computational simulation throughout the CUF encapsulation process at different filling times.

Figure 2 and 3 present the comparison between the flow front profile of experimental works and computational simulation at four distinct filling percentages specifically 20%, 40%, 60% and 80%. This particular case is further emphasized through the data plot of filling time with reference to Figure 2, and 3, the arrangement of beads size among two set of experiments is shown below:

Set		**Size of Beads**	
Layer	**Top**	**Middle**	**Bottom**
A	Small	Medium	Large
B	Large	Small	Medium

Note: Diameter of large, medium and small beads are 5.5mm and 2.9mm respectively.

From the flow front profile shown in Figure 2 and Figure 3 the problem of racing effect is present where the speed of encapsulant varies at different location. At the bumps-free region like central region, it is observed that the flow rate tends to be higher as there is lower resistance to flow whereas flow rate slows down at the bumps region such as the sides of layer, causing the effect of racing effect and possibility of incomplete filling or void formation. Since the orientation of all two sets of experiment are perimeter design, the experimental and computational result are not affected much by the racing effect in terms of filling time and void formation.

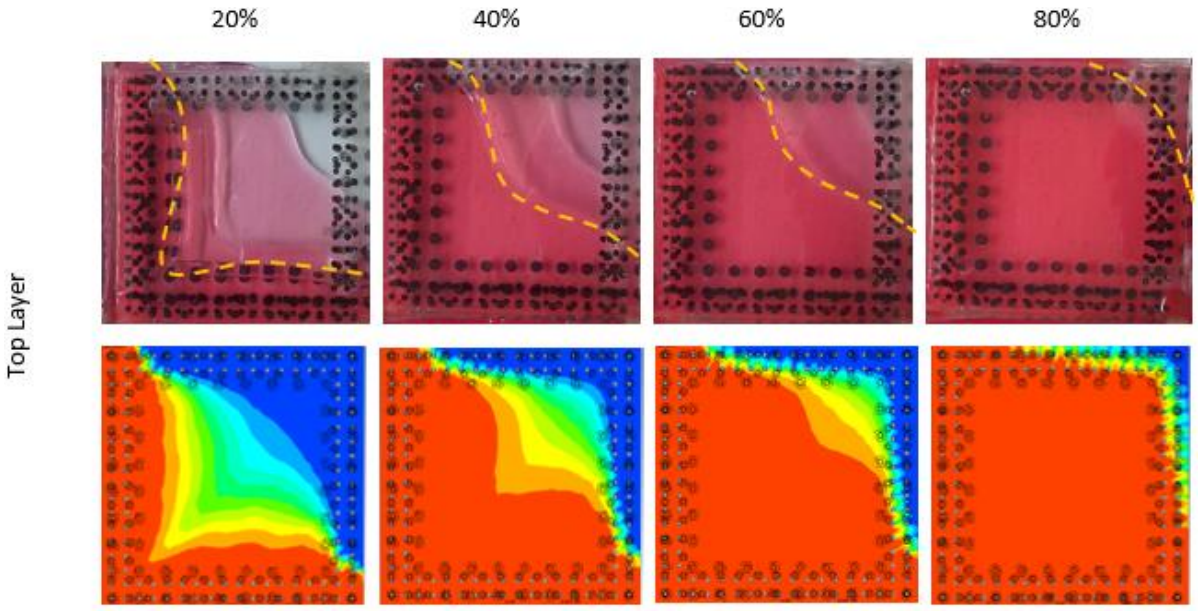

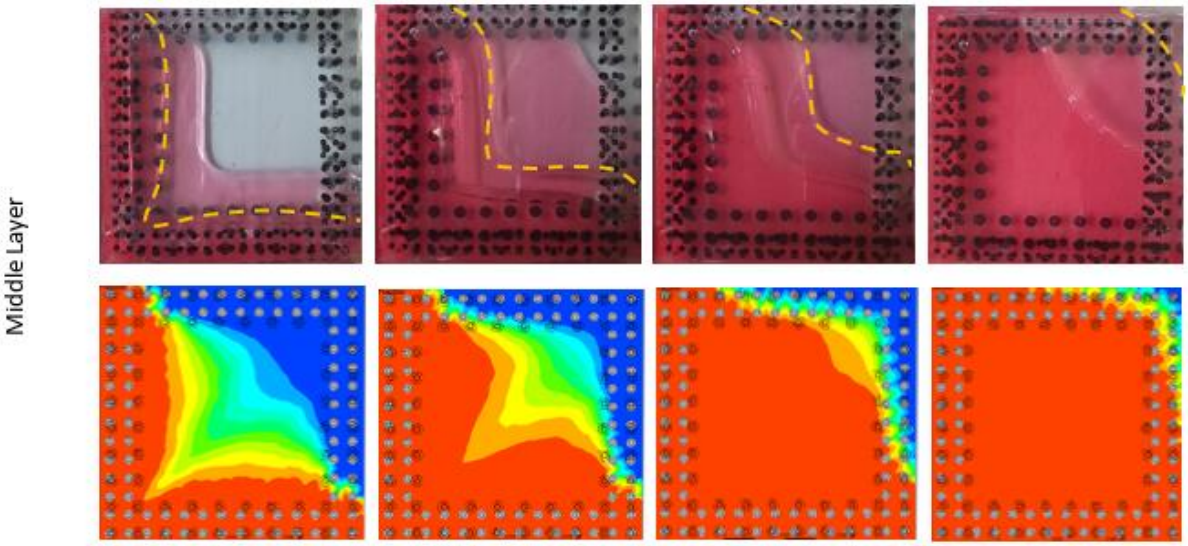

Figure 2: Flow Front Pattern (Experimental vs Simulation) of Set A

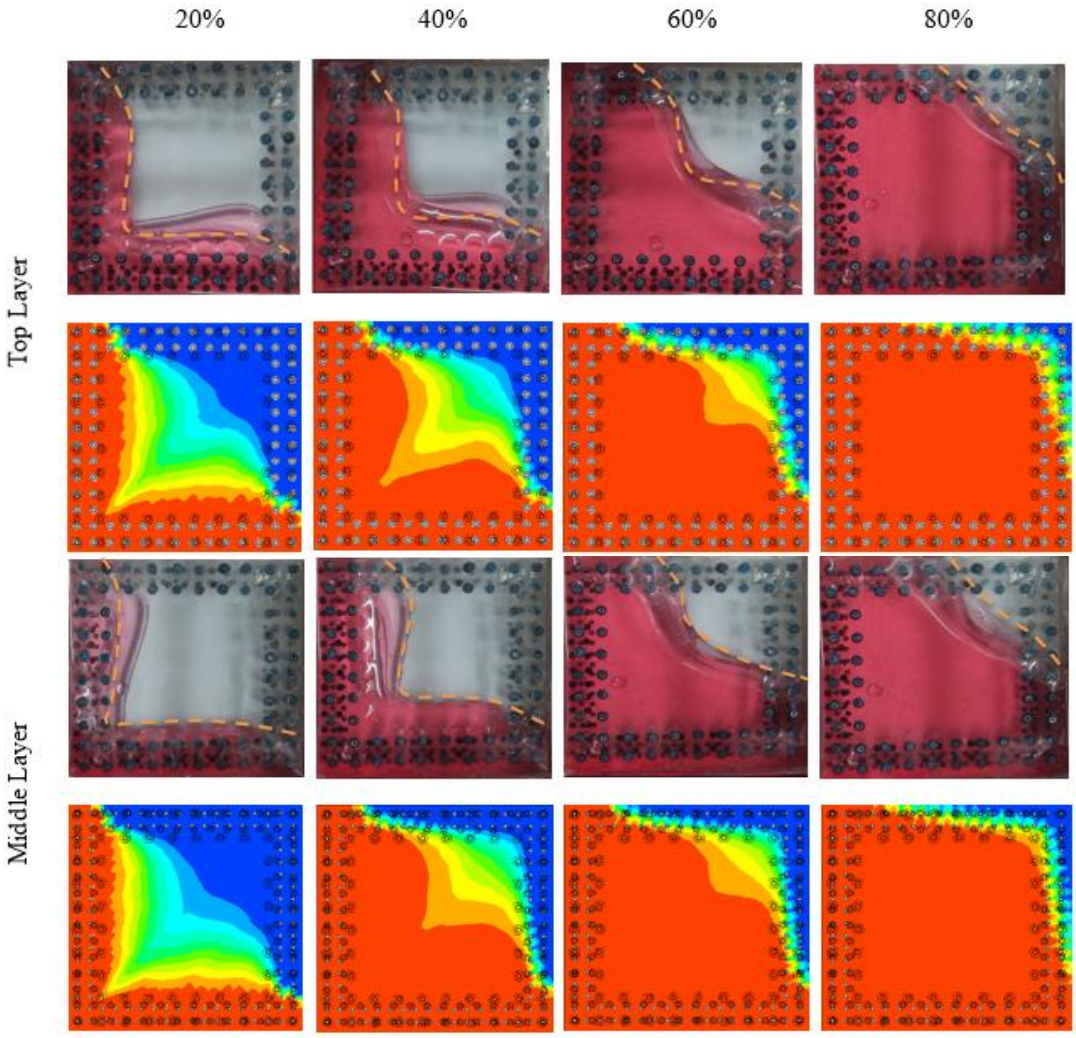

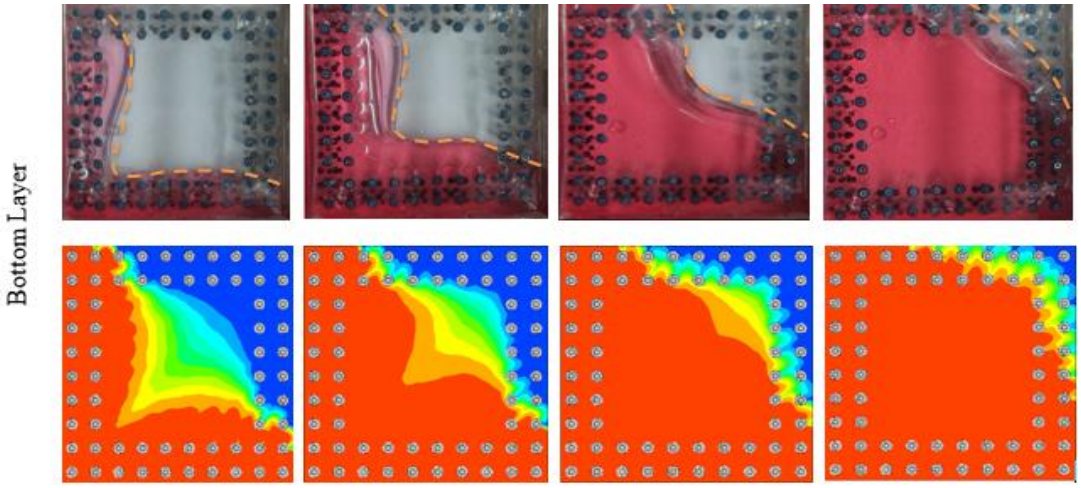

Figure 3: Flow Front Pattern (Experimental vs Simulation) of Set B

3.2. Filling time

According to the experimental and simulation findings, it was found that set A consumes least filling time compared to set B that requires longest time for both layers. Noticeably, longer filling time is expected for larger size of beads as it takes substantial amount of encapsulant to fill up the larger gap height between layers. The filling time for for different percentage of perimeter orientation can be referred to Table 3 and Table 4. Besides, it can be observed that filling rate at set A is very persistant than set B.

Table 3: Experimental filling time

Percentage of filling (%)						
Set	A			B		
Layer	Top	Middle	Bottom	Top	Middle	Bottom
0	0	0	0	0	0	0
20	18	12	6	20	14	17
40	38	25	12	32	22	27
60	57	35	21	42	30	36
80	70	46	31	59	42	46
100	84	59	55	85	60	65

Table 4: Simulation filling time

Percentage of filling (%)						
Set	A			**B**		
Layer	Top	Middle	Bottom	Top	Middle	Bottom
0	0	0	0	0	0	0
20	17	13	8	23	13	19
40	41	28	10	33	24	28
60	58	34	19	42	31	33
80	74	41	29	58	44	40
100	87	57	51	88	59	66

4. Conclusion

This study disclosed the impact of BGA size arrangement filling time, pressure dissemination, and velocity dissemination of CUF encapsulation on BGA packaging. The research was conducted by the approach of experiments and FVM numerical simulations. Two layers of BGA with different sizes (bump diameter of 2.9 and 5.5) in the perimeter orientation are used to determine the best arrangement for constant flow rate and shortest total filling time on L-type dispensing methods. 3-dimensional simulation model with dimensions of 108mm x108mm is generated based on volume of fluid (VOF) method to duplicate the fluid flow phenomenon through BGA which can be used to testify with the data obtained from experiments.

The fluid filling time for BGA size arrangement where the small solders are placed at bottom layer, followed by medium-sized solders and the large solders at the top layer is much faster arrangement since it has smallest gap height to be filled by the fluid at the bottom layer. It also provides the most uniform flow rate at all two layers. Looking at the flow front pattern for all two set of models, it presents a good relation between the experimental works and computational simulation and throughout the CUF encapsulation process at different filling times. Racing effect can be seen as the difference of encapsulant speed at different location. The fluid advances faster in the bump-free region where it has lower resistance to flow, whereas the flow is obstructed by the solder bumps at the bumps region. However, the racing effect is not very obvious and severe for the perimeter orientation.

References

[1] Ardebili H and Pecht M G 2009 Encapsulation Technologies for Electronic Applications. *Encapsulation Technologies for Electronic Applications* Elsevier 129–179 p

[2] Gannamani R and Pecht M 1996 An experimental study of popcorning in plastic encapsulated microcircuits *IEEE Trans Components Packag Manuf Technol Part A* 19(2) 194–201

[3] Ardebili H and Pecht M G 2009 Chapter 3—Encapsulation Process Technology. *In: Encapsulation Technologies for Electronic Applications* Elsevier p 129–79

[4] Khor C Y, Abdullah M Z, Lau C S, Leong W C and Abdul Aziz M S 2014 Influence of solder bump arrangements on molded IC encapsulation *Microelectron Reliab. Elsevier Ltd* 54(4) 796–807

[5] Ong E E, Abdullah M Z, Khor C Y, Leong W C, Loh W K, Ooi C K and Chan R 2013 Numerical Modeling and Analysis of Microbump Pitch Effect in 3D Ic Package With Tsv During Molded

Underfill (Muf) *Eng Appl Comput Fluid Mech* 7(2) 210–22
[6] Wang J 2007 The effects of rheological and wetting properties on underfill filler settling and flow voids in flip chip packages *Microelectron Reliab.* 47(12) 1958–66
[7] Wan J W, Zhang W J and Bergstrom D J 2007 Recent advances in modeling the underfill process in flip-chip packaging *Microelectronics J.* 38(1) 67–75
[8] F C Ng, A Abas, M H H Ishak, M Z Abdullah and M S Abdul Aziz 2016 Effect of thermocapillary action in the underfill encapsulation of multi-stack ball grid array *Microelectronics Reliability 66* 143–160
[9] M Khalil Abdullah, M Z Abdullah, S Kamarudin and Z M Ariff 2007 Study of flow visualization in stacked-Chip Scale Packages (S-CSP) *International Communications in Heat and Mass Transfer 34* 820–828
[10] Ernest E S Ong, M Z Abdullah, C Y Khor, W K Loh, C K Ooi and R Chan 2014 Fluid–structure interaction analysis on the effect of chip stacking in a 3D integrated circuit package with through-silicon vias during plastic encapsulation *Microelectronic Engineering* 113 40–49
[11] Dao-Long C, Tei-Chen C, Ping-Feng Y and Yi-Shao L 2015 Thermal resistance of side by side multi-chip package: Thermal mode analysis *Microelectronics Reliability 55* 822–831
[12] Zienkiewicz O C, Taylor R L and Zhu J Z 2013 The Finite Element Method: its Basis and Fundamentals *Finite Elem Method its Basis Fundam* 493–543
[13] LeVeque R J 2002 Finite Volume Methods for Hyperbolic Problems *publisherName Cambridge University Press*
[14] Morgan M A 1990 1—PRINCIPLES OF FINITE METHODS IN ELECTROMAGNETIC SCATTERING. In: Morgan MABT-FE and FDM in ES, editor *Oxford: Elsevier* p 1–68
[15] Abas A and Abdul-Rahman R 2015 Adaptive FEM with Domain Decomposition Method for Partitioned-Based Fluid–Structure Interaction *Arab J Sci Eng. Springer Berlin Heidelberg* 1–12
[16] Sukop M C and Thorne D T 2006 Lattice boltzmann modeling: An introduction for geoscientists and engineers *Lattice Boltzmann Modeling: An Introduction for Geoscientists and Engineers* p 1–174
[17] Luo L-S 2001 Theory of the Lattice Boltzmann Method: Lattice Boltzmann Models for Non-ideal Gases 62(4) 4982–96
[18] Frisch U and Pazzis D 1986 Lattice as Automata for the Navier-Stokes Equation *Phys Rev Lett.* 1505–8 PMID: 10032689
[19] Mohammed A A 2012 Lattice Boltzmann Method: Fundamentals and Engineering Applications with Computer Codes *AIAA Journal* New York: Springer; 238 p
[20] Bailey C 2005 Numerical modelling for electronic packaging—future requirements *6th Int Conf Electron Packag Technol* 5–6
[21] Chen S and Doolen G D 1998 Lattice Boltzmann method for fluid flows. Annual Review of Fluid Mechanics p 329–64
[22] He X and Doolen G D 2002 Thermodynamic foundations of kinetic theory and Lattice Boltzmann models for multiphase flows *J Stat Phys* 107(1–2) 309–28
[23] Deepak M 2007 VOF based Multiphase Lattice Boltzmann Method using Explicit Kinematic Boundary Conditions at the interface *Georgia Institute of Technology*
[24] Khor C Y, Abdullah M Z, Abdullah M K, Mujeebu M A, Ramdan D, Majid M F M A, Ariff Z M and Rahman M A 2011 Numerical analysis on the effects of different inlet gates and gap heights in TQFP encapsulation process *International Journal of Heat and Mass Transfer* 54(9-10) pp1861-1870
[25] Khor C Y and Abdullah M Z Feb 2013 Analysis of fluid/structure interaction: Influence of silicon chip thickness in moulded packaging *Microelectron Reliab. Elsevier Ltd* 53(2) 334–47
[26] Khor C Y, Abdullah M Z, Che Ani F 2011 Study on the fluid/structure interaction at different inlet pressures in molded packaging *Microelectron Eng. Elsevier B.V* 88(10) 3182–94
[27] Khor C Y, Abdullah M Z, Abdul Mujeebu M and Che Ani F 2010 FVM based numerical study

on the effect of solder bump arrangement on capillary driven flip chip underfill process *Int Commun Heat Mass Transf.* 37(3) 281–6

[28] Orlandini E, Swift M R and Yeomans J 1995 A Lattice Boltzmann Model of Binary-Fluid Mixtures *Europhys Lett* 463

[29] Swift M, Orlandini E, Osborn W and Yeomans J 1996 Lattice Boltzmann simulations of liquid-gas and binary fluid systems *Phys Rev E* 54(5) 5041–52

[30] Zheng H W, Shu C and Chew Y T 2006 A lattice Boltzmann model for multiphase flows with large density ratio *J Comput Phys.* 218(1) 353–71

[31] Yan B and Yan G 2011 A steady-state lattice Boltzmann model for incompressible flows ☆. *Comput Math with Appl. Elsevier Ltd* 61(5) pp 1348–54

[32] Schmieschek S and Harting J 2001 Contact angle determination in multicomponent lattice Boltzmann simulations. Commun Comput Phys. 9:1165

[33] Gunstensen A K, Rothman D H, Zaleski S and Zanetti G 1991 Lattice Boltzmann model of immiscible fluids *Phys Rev A* 43(8) pp 4320–7 PMID: 9905534

[34] Lishchuk S V, Care C M and Halliday I 2003 Lattice Boltzmann algorithm for surface tension with greatly reduced microcurrents *Phys Rev E Stat Nonlin Soft Matter Phys* 67:036701. PMID: 12689196.